

Analytic structure of the Landau gauge gluon propagator

Stefan Strauss,¹ Christian S. Fischer,¹ and Christian Kellermann²

¹*Institut für Theoretische Physik, Justus-Liebig-Universität Gießen,
Heinrich-Buff-Ring 16, D-35392 Gießen, Germany*

²*Institut für Kernphysik, Technische Universität Darmstadt, Schlossgartenstraße 9, 64289 Darmstadt
(Dated: November 27, 2024)*

The analytic structure of the non-perturbative gluon propagator contains information on the absence of gluons from the physical spectrum of the theory. We study this structure from numerical solutions in the complex momentum plane of the gluon and ghost Dyson-Schwinger equations in Landau gauge Yang-Mills theory. The resulting ghost and gluon propagators are analytic apart from a distinct cut structure on the real, timelike momentum axis. The propagator violates the Osterwalder-Schrader positivity condition, confirming the absence of gluons from the asymptotic spectrum of the theory.

Introduction

One of the fundamental properties of QCD is the absence of its elementary degrees of freedom, the quarks and gluons, from the physical spectrum of the theory. The associated problem of quark confinement is a much debated issue [1]. In this discussion it is useful to distinguish between two notions of confinement. One is in terms of color confinement, i.e. the absence of colored states from the asymptotic, physical state space of the theory. The other is strictly related to the center symmetry of Yang-Mills theory. Both notions are not equivalent. If center symmetry is unbroken, there exists a linear rising potential between static color charges in the fundamental representation of the gauge group, stretching out to arbitrary distances r of the charges. In QCD, the mere presence of fundamental dynamical charges breaks this symmetry. Consequently, string breaking sets in at a sufficiently large separation R of the fundamental test charges and the potential becomes flat for $r > R$. Thus, if confinement is defined in terms of unbroken center symmetry, QCD is not a confining theory [1]. Gluons are also not confined in this sense, since they live in the adjoint representation of the gauge group. When two gluons are separated far enough from each other they pull two additional gluons out of the vacuum and dress up to form colorless bound states. This brings us back to the other notion of confinement: the absence of colored asymptotic states. A possible explanation of this absence are positivity violations. By definition, the asymptotic Hilbert space \mathcal{H}_{phys} of colorless physical particles has to be positive (semi-)definite, otherwise a probabilistic interpretation of its S-matrix elements would not be possible. Thus, positivity violations in the gluon propagator constitute a sufficient signal for the absence of gluons from the asymptotic spectrum of the theory.

Another source of interest in the analytic structure of the gluon propagator comes from Heavy-

Ion collisions. Currently, there is great activity both from theory and experiment at RHIC and ALICE/LHC to shed light on the properties of the quark-gluon plasma (QGP), i.e. strongly interacting matter at large temperatures and/or density. Transport models like the Parton-Hadron-String Dynamics approach (PHSD) [2] analyze the dynamics of quarks and gluons in the QGP. An important input into these calculations is the temperature dependent spectral function of the gluon, a quantity directly related to its analytical structure. Whether and how this structure changes below and above the deconfinement transition is currently an open question [3].

How can the zero temperature analytic structure of the gluon propagator look like? Based on studies of the gauge fixing problem, Gribov [4] and later on Zwanziger [5] suggested a form for the gluon propagator with complex conjugate poles at purely imaginary squared Euclidean momenta. A generalization with complex conjugate poles in the negative half-plane of squared complex momenta has been suggested by Stingl in Ref. [6] and has been recently explored in detail in the Refined Gribov-Zwanziger framework Ref. [7]. These forms have in common that they may pose a problem for the analytic continuation of the theory from Minkowski space to the Euclidean formulation used by lattice gauge theory and functional methods. Furthermore, in their pure form they do not account for the perturbative, logarithmic running of the propagator in the large momentum region. An alternative form with a branch cut structure for real and time-like squared momenta has been proposed in Ref. [8] and found to compare well with numerical results for the propagator and its Schwinger functions in the Dyson-Schwinger (DSE) approach.

All explicit calculations of the gluon propagator so far have been restricted to the real and space-like Euclidean momentum domain. Clearly, in order to pin down the analytic structure of the gluon

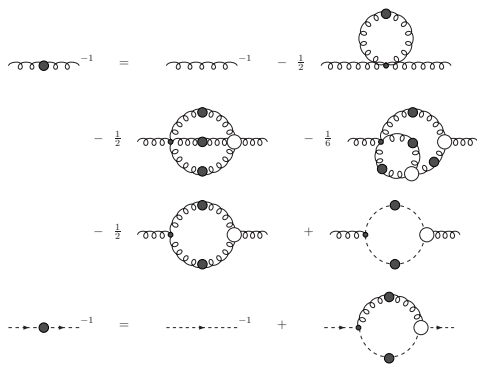


FIG. 1: Dyson-Schwinger equations for the gluon and ghost propagator. Filled circles denote dressed propagators and empty circles denote dressed vertex functions.

propagator, an extension of these calculations into the complex momentum domain is highly desirable. In this letter we report the first results of such a calculation. Within the continuum formulation of Landau gauge Yang-Mills theory we solved the coupled system of Dyson-Schwinger equations for the non-perturbative gluon and ghost propagators in the complex momentum plane and extract the analytic structure at time-like momenta. As a main result we find analytic propagators everywhere, apart from cuts on the real, timelike momentum axis.

The framework

The Dyson-Schwinger equations (DSEs) for the ghost and gluon propagators are shown in Fig. 1. They form a coupled set of integral equations with renormalized, bare and dressed propagators and vertices. In Landau gauge, the explicit form of the propagators is given by

$$\begin{aligned} D_{\mu\nu}(p) &= \left(\delta_{\mu\nu} - \frac{p_\mu p_\nu}{p^2} \right) \frac{Z(p^2)}{p^2} \\ D_G(p) &= -\frac{G(p^2)}{p^2} \end{aligned} \quad (1)$$

with the gluon dressing function $Z(p^2)$ and the ghost dressing function $G(p^2)$. These functions can be numerically determined from their DSEs provided explicit expressions for the dressed ghost-gluon, three-gluon and four-gluon vertices are known. Since these satisfy their own DSEs containing unknown higher n-point functions, in practice one needs to truncate this tower to generate a closed and solvable system of equations. Certainly, meaningful results can only be achieved by careful control of the quality of such a truncation.

A scheme which maintains multiplicative renormalizability and transversality has been devised in Ref. [9]; for transverse projection of the gluon DSE

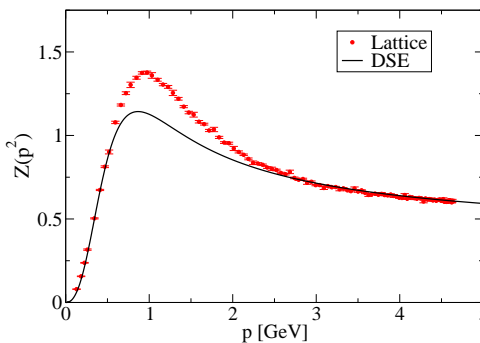


FIG. 2: Results for the gluon dressing function $Z(p^2)$ from lattice calculations [12] compared to the result from DSEs [9].

this scheme is equivalent to the one used previously in Ref. [10]. It uses a bare ghost-gluon vertex, a choice which is close to the results of corresponding lattice calculations [11], an ansatz for the dressed three-gluon vertex in terms of the propagator functions, see [9, 10] for details, and a vanishing four-gluon interaction. Given this choice, the coupled system of DSEs can be solved numerically. The resulting solution for the gluon dressing function $Z(p^2)$ has been discussed in Refs. [9, 10] and, for the convenience of the readers, is shown again in Fig. 2 together with corresponding lattice results [12]. In the large momentum region, where the perturbative behavior sets in, both approaches agree very well. This is also true in the low momentum region. In the deep infrared, the gluon dressing function displays the 'massive' behavior $Z(p^2) \sim p^2$. Such 'decoupling' type of solutions, as opposed to 'scaling' [13], have been suggested long ago [14] and have been revived in Refs. [15–17]. Large volume lattice results agree with this type of solutions [18], although it remains a matter of current debate whether problems with gauge fixing in the context of Gribov copies are already well under control [19–22].

In the mid-momentum region around one GeV there are differences between the DSE and the lattice result on the twenty percent level which have to be attributed to the above discussed vertex truncations for the ghost-gluon, three-gluon and four-gluon vertex. Improvements for the dressed ghost-gluon vertex have been discussed in Refs. [23, 24]. Furthermore, first studies of other types of ansatzes for the dressed three-gluon vertex are available [24] and studies in the background gauge Pinch-technique scheme emphasize the importance of poles in the longitudinal parts of the three-gluon vertex, see [25] for a review. While all these studies are interesting on systematic grounds, the resulting solutions for the gluon

dressing function are not closer to the lattice result than the one shown in Fig. 2. The remaining difference may therefore very well be attributed to the missing two-loop diagrams involving the four-gluon interaction. Indeed, pointwise agreement with the lattice data has been achieved within the framework of functional renormalisation group equations [9], where such contributions can be taken into account due to the exact one-loop structure of the equations. Within the DSE framework the technical complications arising from the two-loop diagrams only allowed for phenomenological treatments of these contributions so far [26], and we therefore prefer to defer a study of the influence of these terms to future work.

The numerical techniques necessary to solve a coupled set of DSEs in the complex plane have been explored up to now only in the context of the fermion propagator, see [27] and the appendix of [8]. The basic idea is to shift the contour of radial integration in the loop integral into the complex plane such that singularities in the angular integral are meliorated. For this work we adapted this method for the ghost and gluon system. Details will be given elsewhere. We have cross-checked our numerics also by employing a different method which solves the DSEs directly on a grid of complex momenta without any shifts in the integrals [28]. The results of both methods agree well for a large range of complex momenta. However, close to the timelike momentum axis, our first method clearly delivered much more stable results and is therefore to be preferred.

Results and discussion

Our results for the analytic structure of the gluon and ghost propagator in SU(N) Yang-Mills theory are shown in Figs. 3 and 4. Let us first discuss the real parts of the propagators. In the lower diagram of Fig. 3 we see a spike structure of the ghost dressing function, which is located at the origin of the complex momentum plane. Since we have chosen a decoupling type of solution for the ghost-gluon system, the ghost dressing function is finite at $p^2 = 0$. At our numerical infrared cut-off $|\epsilon^2| = 10^{-5}$ the value $G(\epsilon^2)$ depends slightly on the direction from which zero is approached. In our calculation $G(\epsilon^2) = 5$ when $p^2 \rightarrow 0^+$, but $G(-\epsilon^2) = 5.005 \mp i0.004$ when $p^2 \rightarrow 0^-$ on the real axis. Thus, the real part of the ghost dressing function is almost symmetric around the origin of the complex momentum plane. For the real part of the gluon propagator in the upper diagram of Fig. 3 the situation is entirely different. Again, the propagator is finite at $p^2 = 0$ but shows large positive values for complex momenta and negative structures close to the negative real momentum axis.

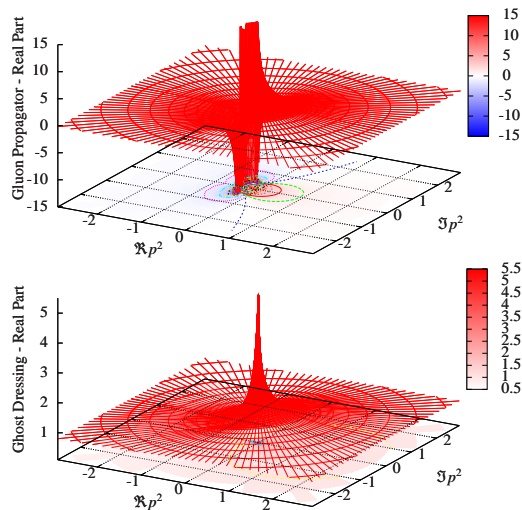


FIG. 3: Results for the real part of the gluon propagator function $D(p^2)$ and the ghost dressing function $G(p^2)$ in the complex momentum plane including colored contour maps and lines. The displayed range of the gluon propagator is restricted in order to resolve smaller structures. See text for the extrema of $\Re D(p^2)$.

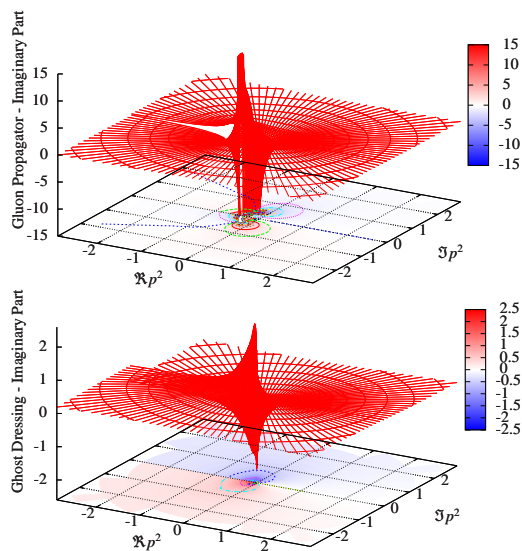


FIG. 4: Results for the imaginary part of the gluon propagator function $D(p^2)$ and the imaginary part of the ghost dressing function $G(p^2)$ in the complex momentum plane including colored contour maps and lines. The displayed range of the gluon propagator is restricted in order to resolve smaller structures. See also Fig. 5 for the full scale.

The positive spikes extend up to $\Re D(p^2) = 40$ GeV² staying definitely finite. Closer to the negative real momentum axis the propagator becomes negative for $|p^2|$ larger than some finite value on the negative real momentum axis. The corresponding narrow dip is finite in depth and sizably extends 0.3 GeV² out into the complex momentum

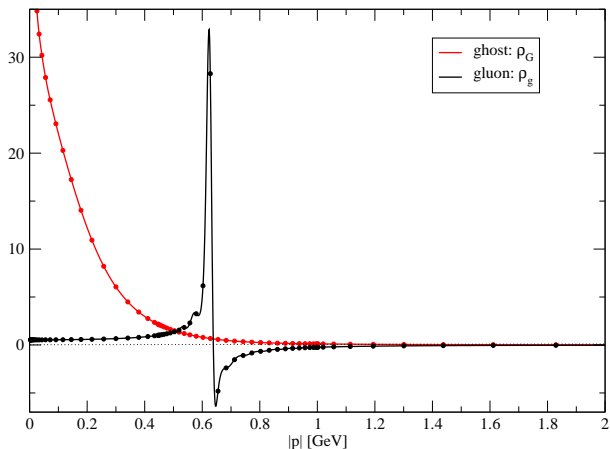


FIG. 5: Results for the gluon spectral function and the ghost spectral function as a function of momentum.

plane. The minimum value of the dip is approximately $\Re D(p^2) = -105 \text{ GeV}^2$.

Now let us discuss the imaginary part in Fig. 4. Here we clearly see a cut-structure emerging for both, the gluon propagator and the ghost dressing function along the negative real momentum axis. No further structure is seen in the complex momentum plane. We thus arrive at an important result of our study: the ghost and gluon propagators have nontrivial analytic structure only on the timelike real momentum axis. This is in contrast to the expectations from the studies of Gribov, Zwanziger and Stingl [4–7], which all assumed singularities away from the real momentum axis. We find no evidence for these. Within the present numerical accuracy, the cuts are sharply peaked but finite. Whether an even more precise treatment leads a singularity in $\Im D(p^2)$, as assumed in the fits to the DSE results in Ref. [8], remains an open question.

The cuts in the imaginary part of the ghost and gluon propagators are directly related with the corresponding spectral functions,

$$\rho_{G,g}(p^2) = -\Im\{D_{G,g}(p^2)\}/\pi \quad (2)$$

with $D_G(p^2) = -G(p^2)/p^2$, $D_g(p^2) = Z(p^2)/p^2$ and the momentum p^2 on the negative real momentum axis of the upper complex half plane. We therefore show them more closely in Fig. 5. Our numerical results are obtained on a grid of momentum points which are displayed explicitly, whereas the interpolation is done via Chebychev polynomials and serves to guide the eye. For the ghost spectral function (and most of the gluon) this interpolation clearly works also on a quantitative level; however, the interpolation for the gluon in the region $0.5 < |p| < 0.7 \text{ GeV}$ can only be regarded as a qualitative one. Whereas the ghost spectral function is

dominated by the massless $1/p^2$ pole in the propagator, the gluon is clearly different. Its imaginary part rises first, turns over and crosses through zero, turns again and then approaches zero from below at large timelike momenta. The exact locations and heights of the maxima in the positive and negative region cannot be determined precisely within the present numerical accuracy. Nevertheless, the qualitative behavior is fixed from the explicitly calculated points shown in the plot. The gluon spectral function obeys the Oehme-Zimmermann normalization condition [29]

$$Z_3^{-1} = \int \rho_g(s) ds, \quad (3)$$

where Z_3 denotes the gluon wave function renormalization constant, with a deviation of 10 percent. This provides a measure on the accuracy achieved in the present computation. The negative contributions to the gluon spectral function indicate its absence from the asymptotic spectrum of the theory. In general, the cuts in the ghost and gluon propagators signal the radiation of unphysical particles (ghosts and gluons) from unphysical particles. Moreover, the gluon is certainly not a massive particle in the usual sense. Nevertheless one may be tempted to define something like an "effective mass" m_g for the gluon from the location of the positive peak in the spectral function. Within the present accuracy we find

$$600 \text{ MeV} < m_g < 700 \text{ MeV}. \quad (4)$$

We stress again, however, that m_g is not a measurable quantity; strictly speaking, it is just the scale where positivity violations in the gluon set in.

In this work we presented the first non-perturbative solution of the gluon and ghost propagators in the complex momentum plane together with an extraction of their respective spectral functions. We presented results for the decoupling case; a comprehensive comparison with scaling will be given elsewhere. Besides the considerable theoretical interest in these functions they are also a necessary input into the calculations of glueball masses within the framework of Bethe-Salpeter equations. Corresponding results will be detailed in a subsequent work.

Acknowledgements

We thank Reinhard Alkofer, Jan Pawłowski and Lorenz von Smekal for fruitful discussions. This work has been supported by the Helmholtz Young Investigator Grant VH-NG-332 and the Helmholtz International Center for FAIR within the LOEWE program of the State of Hesse.

-
- [1] J. Greensite, Lect. Notes Phys. **821** (2011) 1.
- [2] W. Cassing and E. L. Bratkovskaya, Nucl. Phys. A **831** (2009) 215 [arXiv:0907.5331 [nucl-th]].
- [3] A. Maas, arXiv:1106.3942 [hep-ph].
- [4] V. N. Gribov, Nucl. Phys. B **139** (1978) 1.
- [5] D. Zwanziger, Nucl. Phys. B **323** (1989) 513.
- [6] M. Stingl, Phys. Rev. D **34** (1986) 3863 [Erratum-ibid. D **36** (1987) 651].
- [7] A. Cucchieri, D. Dudal, T. Mendes and N. Vandersickel, Phys. Rev. D **85** (2012) 094513 [arXiv:1111.2327 [hep-lat]].
- [8] R. Alkofer, W. Detmold, C. S. Fischer and P. Maris, Phys. Rev. D **70** (2004) 014014 [hep-ph/0309077]; Nucl. Phys. Proc. Suppl. **141** (2005) 122 [hep-ph/0309078].
- [9] C. S. Fischer, A. Maas, J. M. Pawłowski, Annals Phys. **324** (2009) 2408-2437.
- [10] C. S. Fischer, R. Alkofer, Phys. Lett. B **536** (2002) 177.
- [11] A. Cucchieri, A. Maas and T. Mendes, Phys. Rev. D **77** (2008) 094510 [arXiv:0803.1798 [hep-lat]].
- [12] A. Sternbeck, E. M. Ilgenfritz, M. Müller-Preussker, A. Schiller and I. L. Bogolubsky, PoS **LAT2006**, 076 (2006) [arXiv:hep-lat/0610053].
- [13] P. Watson and R. Alkofer, Phys. Rev. Lett. **86** (2001) 5239 [hep-ph/0102332]. C. Lerche, L. von Smekal, Phys. Rev. D **65** (2002) 125006; D. Zwanziger, Phys. Rev. D **67**, 105001 (2003); J. M. Pawłowski, D. F. Litim, S. Nedelko and L. von Smekal, Phys. Rev. Lett. **93**, 152002 (2004); R. Alkofer, C. S. Fischer and F. J. Llanes-Estrada, Phys. Lett. B **611**, 279 (2005); C. S. Fischer and J. M. Pawłowski, Phys. Rev. D **75**, 025012 (2007); Phys. Rev. **D80** (2009) 025023.
- [14] J. M. Cornwall, Phys. Rev. D **26** (1982) 1453.
- [15] A. C. Aguilar, D. Binosi and J. Papavassiliou, Phys. Rev. D **78** (2008) 025010.
- [16] Ph. Boucaud, *et al.* JHEP **0806**, 012 (2008); JHEP **0806**, 099 (2008).
- [17] D. Dudal, J. A. Gracey, S. P. Sorella, N. Vandersickel and H. Verschelde, Phys. Rev. D **78**, 065047 (2008).
- [18] A. Cucchieri and T. Mendes, Phys. Rev. D **78** (2008) 094503; Phys. Rev. Lett. **100**, 241601 (2008). I. L. Bogolubsky *et al.*, Phys. Lett. **B676** (2009) 69.
- [19] L. von Smekal, arXiv:0812.0654 [hep-th].
- [20] A. Sternbeck, L. von Smekal, Eur. Phys. J. **C68** (2010) 487; A. Maas *et. al.*, Eur. Phys. J. C **68** (2010) 183.
- [21] A. Cucchieri and T. Mendes, Phys. Rev. D **81** (2010) 016005 [arXiv:0904.4033 [hep-lat]].
- [22] A. Maas, Phys. Lett. **B689** (2010) 107.
- [23] P. Boucaud, D. Dudal, J. P. Leroy, O. Pene and J. Rodriguez-Quintero, JHEP **1112** (2011) 018 [arXiv:1109.3803 [hep-ph]].
- [24] M. R. Pennington and D. J. Wilson, Phys. Rev. D **84** (2011) 119901 [arXiv:1109.2117 [hep-ph]].
- [25] D. Binosi and J. Papavassiliou, Phys. Rept. **479** (2009) 1.
- [26] J. C. R. Bloch, Few Body Syst. **33** (2003) 111 [hep-ph/0303125].
- [27] P. Maris, Phys. Rev. D **52** (1995) 6087 [hep-ph/9508323].
- [28] C. Kellermann, Ph.D. thesis, Technische Universität Darmstadt, 2012.
- [29] R. Oehme and W. Zimmermann, Phys. Rev. D **21** (1980) 471.